

# An asymmetric stabilizer based on scheduling shifted coordinates for single-input linear systems with asymmetric saturation

Philipp Braun,<sup>1</sup> Giulia Giordano,<sup>2</sup> Christopher M. Kellett<sup>1</sup> and Luca Zaccarian<sup>2,3</sup>

**Abstract**—Starting from a symmetric state-feedback solution ensuring  $\alpha$ -exponential convergence in an ellipsoidal sublevel set, with asymmetric saturation and single-input linear plants, we propose a novel asymmetric scheduled extension preserving the original symmetric solution in that sublevel set and extending the guaranteed stability region to the union of all possible contractive ellipsoids centered at a shifted equilibrium. Our design being based on the solution of a parametric optimization problem, we prove Lipschitz properties of the ensuing feedback law and we compute its explicit state-feedback expression.

## I. INTRODUCTION

While input saturation has been mostly studied using symmetric limits (see, e.g., [11], [17]), asymmetric limits often arise in practice, thereby making the symmetric solutions (typically based on focusing on the smallest limit) quite conservative. The community started looking into nonsymmetric Lyapunov certificates in the presence of symmetric stabilizers (see [4] and references therein, and also [12], [13]). A piecewise quadratic Lyapunov function with symmetric stabilizing saturated linear feedbacks is used in [14] and [10], in the continuous-time and discrete-time cases, respectively. Symmetrically stabilizing a shifted equilibrium (see [5, Ch. 8] and references therein) comes at the cost of not stabilizing the origin any longer. In [18], a switching dynamical controller is designed to exploit the available range of the control action on both sides of the saturation levels. To provide enlarged basins of attraction, [15] proposes the design of an asymmetric stabilizer, based on the convex scaling in [6] for the shifted stabilizer. That solution provides significantly larger guarantees but has the drawback of 1) restricting the achievable basin of attraction with a conservative point inclusion condition required to apply the technique in [6] and 2) reducing the local performance of the symmetric solution. In model predictive control (MPC), constraints can be directly incorporated in the controller design: explicit MPC can handle linear systems with symmetric or asymmetric input saturation levels in an explicit controller design [3]. However, explicit MPC derives a control law based on discrete-time systems in general, whereas here we address the problem in the continuous-time setting. See [3] or [8] for details on (explicit) MPC.

\* P. Braun and L. Zaccarian are supported in part by the Agence Nationale de la Recherche (ANR) via grant “Hybrid And Networked Dynamical sYstems” (HANDY), number ANR-18-CE40-0010.

<sup>1</sup>School of Engineering, Australian National University, Canberra, Australia. {philipp.braun, chris.kellett}@anu.edu.au

<sup>2</sup>Department of Industrial Engineering, University of Trento, Trento, Italy. giulia.giordano@unitn.it

<sup>3</sup>LAAS-CNRS, Université de Toulouse, Toulouse, France. luca.zaccarian@laas.fr

We propose a novel asymmetric scheme based on focusing on the shifted equilibrium, as in [5, Ch. 8], and continuously driving that equilibrium back to the origin by relying on the solution of a parametric optimization problem. As compared to [15], this solution is not based on convex scalings and therefore preserves the convergence rate given by the symmetric stabilizer in its guaranteed ellipsoidal set. Moreover, it does not require any point inclusion conditions, therefore obtaining an estimate of the basin of attraction containing all the contractive ellipsoids that can be constructed in shifted coordinates. While the proposed framework applies to multi-input plants, we focus most of the paper on the single-input case, for which we can compute explicit expressions of the control law solving the optimization. We discuss symmetric and shifted asymmetric stabilizers in Section II, then for the single-input case we propose our optimization-based solution in Section III and its explicit version in Section IV. Numerical examples in Section V show the ability of our controller to provide greatly enlarged certified stability regions.

**Notation.** For  $u^-, u^+ \in \mathbb{R}_{>0}^m$ ,  $m \in \mathbb{N}$ ,  $\text{sat}_{[u^-, u^+]}(u) = \max\{\min\{u^+, u\}, -u^-\}$  defines the saturation, where the maximum/minimum are to be understood componentwise. The deadzone is defined as  $\text{dz}_{[u^-, u^+]}(u) = u - \text{sat}_{[u^-, u^+]}(u)$ . For  $Z \in \mathbb{R}^{n \times n}$ ,  $\text{He}(\cdot)$  denotes  $\text{He}(Z) = Z + Z^\top$ . For  $Z \in \mathbb{R}^{n \times m}$  and  $z \in \mathbb{R}^n$ ,  $Z_{[k]}$  and  $z_k$  denote the  $k$ -th row and the  $k$ -th entry, respectively. A vector  $v \in \mathbb{R}^n$  satisfies  $v \leq \min\{u^-, u^+\}$  if  $v_k \leq \min\{u_k^-, u_k^+\}$  for all  $k \in \{1, \dots, n\}$ . A positive definite matrix  $P \in \mathbb{R}^{n \times n}$  can be uniquely decomposed as  $P = P^{\frac{1}{2}} P^{\frac{1}{2}}$  where  $P^{\frac{1}{2}} \in \mathbb{R}^{n \times n}$  is positive definite. In  $\mathbb{R}^n$ , we use the norms  $|x| = \sqrt{x^\top x}$ ,  $|x|_P = \sqrt{x^\top P x}$ ,  $P \in \mathbb{R}^{n \times n}$  positive definite,  $I \in \mathbb{R}^{n \times n}$  denotes the identity matrix,  $\mathbb{1}$  satisfies  $\mathbb{1}_k = 1$ ,  $k \in \{1, \dots, n\}$  and  $\text{int}(\mathcal{A})$  denotes the interior of a set  $\mathcal{A} \subset \mathbb{R}^n$ .

## II. SYMMETRIC AND SHIFTED STABILIZERS

We consider linear saturated continuous-time systems

$$\dot{x} = Ax + B \text{sat}_{[u^-, u^+]}(u) \quad (1)$$

with state  $x \in \mathbb{R}^n$ , input  $u \in \mathbb{R}^m$ ,  $A \in \mathbb{R}^{n \times n}$ ,  $B \in \mathbb{R}^{n \times m}$  and saturation limits  $u^-, u^+ \in \mathbb{R}_{>0}^m$ . We define the average saturation range and the average saturation center as

$$\bar{u} = \frac{1}{2}(u^+ + u^-), \quad u_o = \frac{1}{2}(u^+ - u^-). \quad (2)$$

For simplicity, we assume that the average saturation range  $\bar{u}_k$  satisfies  $\bar{u}_k = 1$  for all  $k \in \{1, \dots, m\}$ ; this is not restrictive and can always be assumed without loss of generality for  $u^-, u^+ \in \mathbb{R}_{>0}^m$  by scaling the columns of  $B$ .

*Assumption 1:* It holds that  $\bar{u} = \mathbb{1} \in \mathbb{R}^m$ .  $\diamond$

To convey the idea of the controller design and to obtain explicit formulations, we restrict our presentation in most parts of the paper to the single input case and we assume that the matrix  $A$  is non-singular. However, by discussing different cases and by using a more convoluted notation, the ideas appear to extend to the multi input case and to dynamics (1) with singular matrix  $A$ .

*Assumption 2:* The pair  $(A, B)$  is stabilizable and  $A$  is non-singular.  $\diamond$

Of particular interest is the subspace of induced equilibria

$$\Gamma = \{x_e \in \mathbb{R}^n : Ax_e + Bu_e = 0, u_e \in \mathbb{R}^m\}. \quad (3)$$

Under Assumption 2, there is a continuous mapping  $u_e \mapsto x_e(u_e)$  defined as

$$x_e(u_e) = -A^{-1}Bu_e, \quad (4)$$

characterizing pairs of induced equilibria  $(x_e, u_e) \in \Gamma \times \mathbb{R}^m$  through the input  $u_e \in \mathbb{R}^m$ . In the definition of  $\Gamma$ , the saturation levels are not present. System (1) with  $u \in [-u^-, u^+]$  (to be understood componentwise) can only be stabilized at  $x_e$  if a corresponding input satisfies  $u_e \in (-u^-, u^+)$ .

In a neighborhood of the origin, we seek a feedback law

$$u = Kx + L dz_{[u^-, u^+]}(u), \quad (5)$$

with  $K \in \mathbb{R}^{m \times n}$ ,  $L \in \mathbb{R}^{m \times m}$ , asymptotically stabilizing the origin. Combining (1) and (5), the closed-loop dynamics can be written as

$$\begin{aligned} \dot{x} &= (A + BK)x - (B - BL) dz_{[u^-, u^+]}(u) \\ u &= Kx + L dz_{[u^-, u^+]}(u). \end{aligned} \quad (6)$$

To characterize basins of attraction of asymptotically stable (induced) equilibria  $x_e$ , we consider sublevel sets of quadratic functions. In particular, for  $\kappa \in \mathbb{R}_{\geq 0}$ ,  $x_e \in \mathbb{R}^n$  and  $P \in \mathbb{R}^{n \times n}$  positive definite we define the set

$$\mathcal{E}_x^\kappa(P) = \{x \in \mathbb{R}^n : |x - x_e|_P \leq \kappa\}. \quad (7)$$

*Proposition 1 (Symmetric Stabilizer; [15, Theorem 1]):*

Given the plant (1), let  $v \in \mathbb{R}_{\geq 0}^m$  with  $v \leq \min\{u^-, u^+\}$  and let  $\alpha \in \mathbb{R}_{\geq 0}$ . Moreover, let  $\tilde{Q}_v \in \mathbb{R}^{n \times n}$ ,  $W_v, Y_v \in \mathbb{R}^{m \times n}$ ,  $U_v, X_v \in \mathbb{R}^{m \times m}$  be a solution of the optimization problem

$$\max_{Q, W, Y, U, X} \log \det(Q) \quad (8)$$

subject to  $U > 0$  diagonal,  $Q = Q^\top > 0$

$$\text{He} \begin{bmatrix} AQ + BW + \alpha Q & -BU + BX \\ W + Y & X - U \end{bmatrix} < 0$$

$$\begin{bmatrix} v_k^2 & Y_{[k]} \\ Y_{[k]}^\top & Q \end{bmatrix} \geq 0, \quad k = 1, \dots, m.$$

Then, for

$$K = W_v Q_v^{-1}, \quad L = X_v U_v^{-1}, \quad P_v = Q_v^{-1} \quad (9)$$

the nonlinear algebraic loop in (5) is well posed (i.e., its solution is unique and Lipschitz) and  $x^\top P_v x$  exponentially decreases with rate larger than  $2\alpha$  within the set  $\mathcal{E}_0^1(P_v)$ . Consequently, the origin of (6) is locally exponentially stable, with basin of attraction containing the set  $\mathcal{E}_0^1(P_v)$ .  $\lrcorner$

The subscript  $v$  is used to indicate the dependence of  $P$  on the selection of vector  $v \in \mathbb{R}_{\geq 0}^m$ . In particular, we observe that LMIs (8) are homogeneous in the decision variables, except for  $v_k^2$  in the constraints. Therefore, scaling

vector  $v$  in Proposition 1 by a positive scalar  $\kappa$  leads to scaling the corresponding optimal solution (8) by  $\kappa^2$ . More specifically, according to (9), this corresponds to a scaled  $P_{\kappa v} = \kappa^{-2}P_v$ , whereas gains  $K$  and  $L$  remain unchanged because the scaling cancels out (this is the reason why no subscript is used in  $K$  and  $L$ ). Finally, the certified ellipsoidal set scales from  $\mathcal{E}_0^1(P_v)$  to  $\mathcal{E}_0^1(P_{\kappa v}) = \mathcal{E}_0^\kappa(P_v)$ . This fact is stated in the next corollary.

*Corollary 1 (Homogeneity):* Let  $K, L, P_v$  defined in (9) correspond to an optimal solution of (8) for  $v \in \mathbb{R}_{\geq 0}^m$ . Then for all  $\kappa \in \mathbb{R}_{\geq 0}$  with  $\kappa v \leq \min\{u^-, u^+\}$ , and with the same gains  $K$  and  $L$ , function  $x^\top P_v x$  exponentially decreases with rate larger than  $2\alpha$  within the set  $\mathcal{E}_0^\kappa(P_v)$ .  $\lrcorner$

Proposition 1 can be used to define a control law stabilizing an induced equilibrium, instead of the origin. Consider an equilibrium pair  $(x_e, u_e)$  satisfying (4) and assume that  $u^- + u_e, u^+ - u_e \in \mathbb{R}_{> 0}^m$ . Additionally, consider the coordinate transformation  $\tilde{x} = x - x_e$  and  $\tilde{u} = u - u_e$ . It holds that

$$\begin{aligned} \dot{\tilde{x}} &= \dot{x} = Ax + B \text{sat}_{[u^-, u^+]}(u) \\ &= A\tilde{x} + Ax_e + B(u_e + \text{sat}_{[u^- + u_e, u^+ - u_e]}(\tilde{u})) \\ &= A\tilde{x} + B \text{sat}_{[u^- + u_e, u^+ - u_e]}(\tilde{u}). \end{aligned} \quad (10a)$$

with the shifted input  $\tilde{u}$  selected as follows

$$\tilde{u} = K\tilde{x} + L dz_{[u^- + u_e, u^+ - u_e]}(\tilde{u}). \quad (10b)$$

For the shifted dynamics (10), the same result as that of Corollary 1 applies. This fact is stated in the following corollary, where a more convenient expression of  $u$  is deduced from (10b) exploiting the identities (4) and  $dz_{[u^- + u_e, u^+ - u_e]}(\tilde{u}) = dz_{[u^-, u^+]}(u)$ , which follows straightforwardly from (10a).

*Corollary 2:* Let Assumption 2 be satisfied. Consider an equilibrium pair  $(x_e, u_e)$  defined through (4). Given  $\kappa \in \mathbb{R}_{> 0}$  and  $v \in \mathbb{R}_{\geq 0}^m$  assume that  $\kappa v \leq \min\{u^- + u_e, u^+ - u_e\}$ , and let  $K, L, P_v$  defined in (9) correspond to an optimal solution of (8). Then the following selection of the input  $u$

$$u = u_e + K(x + A^{-1}Bu_e) + L dz_{[u^-, u^+]}(u) \quad (11)$$

ensures that function  $V_{x_e} : \mathbb{R}^n \rightarrow \mathbb{R}_{\geq 0}$

$$V_{x_e}(x) = (x - x_e)^\top P_v (x - x_e) = |x - x_e|_{P_v}^2 = |\tilde{x}|_{P_v}^2 \quad (12)$$

exponentially decreases with rate larger than  $2\alpha$ , i.e.,

$$\langle 2P_v(x - x_e), Ax + B \text{sat}_{[u^-, u^+]}(u) \rangle < -2\alpha V_{x_e}(x), \quad (13)$$

within the sublevel set  $\tilde{x} \in \mathcal{E}_0^\kappa(P_v)$ . Consequently, selection (11) locally exponentially stabilizes the (induced) equilibrium  $x_e(u_e)$  of (1), as per (4), with basin of attraction containing the shifted ellipsoid  $\mathcal{E}_{x_e}^\kappa(P_v)$  defined in (7).  $\lrcorner$

*Remark 1:* Expression (11) specifies the control input  $u$  only implicitly, even though Proposition 1 ensures that the corresponding solution is Lipschitz. Proceeding as in [15, Lemma 3], for the single-input case  $m = 1$ , the selection

$$\begin{aligned} u &= u_e + K(x + A^{-1}Bu_e) \\ &\quad + L(I - L)^{-1} dz_{[u^-, u^+]}(u_e + K(x + A^{-1}Bu_e)) \end{aligned} \quad (14)$$

can be proven to be the explicit solution to (11).  $\circ$

Note that an appropriate coordinate transformation  $x \mapsto P_v^{\frac{1}{2}}x$ , i.e.,

$$\chi = P_v^{\frac{1}{2}}x \iff x = (P_v^{\frac{1}{2}})^{-1}\chi, \quad (15)$$

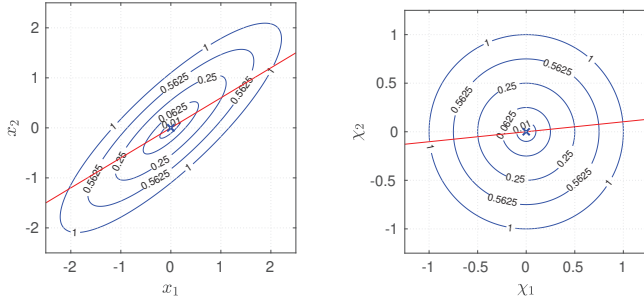


Fig. 1. Level sets of the function  $V(x) = x^\top P_1 x$  in the original coordinates (left) and in the rotated coordinates  $\chi = P_1^{\frac{1}{2}} x$  (right). Additionally, the subspace of induced equilibria (3) is shown in red.

with  $P_v^{\frac{1}{2}} \in \mathbb{R}^{n \times n}$  symmetric and positive definite, allows us to consider, instead of the Lyapunov function with ellipsoidal level sets, a Lyapunov function with circular level sets. Using the notation introduced in the results discussed in this section, the function (12) reduces to the Euclidean norm in the  $\chi$ -coordinates,  $\hat{V}_{\chi_e} : \mathbb{R}^n \rightarrow \mathbb{R}_{\geq 0}$ ,  $\hat{V}_{\chi_e}(\chi) = |\chi - \chi_e|^2$ . With  $C := P_v^{\frac{1}{2}} A^{-1} B$ , induced equilibria (4) are given by

$$\chi_e(u_e) = P_v^{\frac{1}{2}} x_e(u_e) = -P_v^{\frac{1}{2}} A^{-1} B u_e \quad (16)$$

in the  $\chi$ -coordinates. While using coordinates  $\chi$  instead of  $x$  is not necessary in the following sections, the interpretations in the  $\chi$ -coordinates are more illustrative in some places.

*Example 1:* Consider the dynamical system (1) defined through the matrices  $A = \begin{bmatrix} 0.6 & -0.5 \\ 0.3 & 1.0 \end{bmatrix}$  and  $B = \begin{bmatrix} 1 \\ 3 \end{bmatrix}$ . Solving (8)<sup>1</sup> the positive definite matrix  $P_1 = Q_1^{-1} = \begin{bmatrix} 0.7399 & -0.6654 \\ -0.6654 & 0.8266 \end{bmatrix}$  is obtained for  $v = 1$  and  $\alpha = 0.1$ . In Fig. 1 the level sets of the function  $V(x) = x^\top P_1 x$  and  $\hat{V}(\chi) = \chi^\top \chi$  are shown on the left and on the right, respectively. Here, we obtain  $P_1^{\frac{1}{2}} = \begin{bmatrix} 0.7447 & -0.4305 \\ -0.4305 & 0.8008 \end{bmatrix}$ . In addition, the subspace of induced equilibria  $\Gamma$  defined in (3) is shown in red in Fig. 1. Since  $v = 1$ , if  $\kappa \leq \min\{u^-, u^+\}$  for  $\kappa \in \mathbb{R}_{>0}$ , then the origin of the closed-loop system (6) is asymptotically stable and the domain of attraction contains the set  $\mathcal{E}_0^\kappa(P_1)$  according to Proposition 1 and Corollary 1.

Assume now that the saturation levels are fixed at  $u^- = 1.5$  and  $u^+ = 0.5$ . Then Proposition 1 and Corollary 1 can be applied with  $v = 1$  and  $\kappa = 0.5$  guaranteeing that the blue sublevel set in Fig. 2 is contained in the basin of attraction of the closed-loop system (6). Alternatively, the sublevel sets

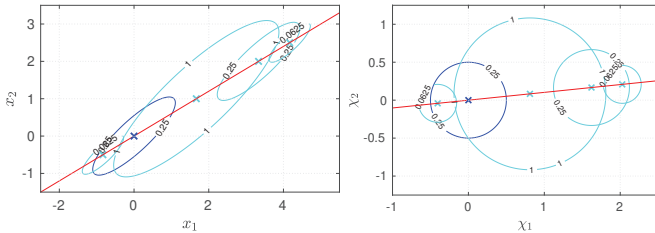


Fig. 2. Sublevel sets  $\mathcal{E}_{x_e}^\kappa(P)$  for different (induced) equilibria for which the combination of Proposition 1 and Corollaries 1 and 2 guarantee asymptotic stability of the (induced) equilibrium  $x_e$  of the closed-loop system.

<sup>1</sup>To avoid numerical problems, the absolute values of unknowns in (8) are additionally constrained to be less or equal to 10. Here, (8) is solved through CVX [9] in Matlab.

guaranteeing asymptotic stability of the induced equilibria  $x_e = -A^{-1} B u_e$ ,  $u_e \in (-1.5, 0.5)$ , using the feedback law (11) can be derived through Corollary 2. For  $u_e = -0.5$ , the assumptions of Corollary 2 are satisfied for  $\kappa = 1$ , leading to a larger sublevel set  $\mathcal{E}_{x_e(u_e)}^1(P_1)$ , compared with  $\mathcal{E}_0^{0.5}(P_1)$ , for which convergence to  $x_e$  is guaranteed (see Fig. 2).  $\diamond$

### III. OPTIMIZATION-BASED SHIFTED STABILIZER

Fig. 2 and the discussions above clearly indicate that the size of the estimate of the basin of attraction varies significantly with the induced equilibrium to be stabilized. We exploit here this potential by deriving a modified controller with a larger estimate of the basin of attraction. In particular, the basin of attraction of our modified feedback law includes all sublevel sets  $\mathcal{E}_{x_e(u_e)}^\kappa(P_1)$ ,  $u_e \in (-u^-, u^+)$ , for which asymptotic stability of  $x_e$  is guaranteed through Proposition 1, Corollaries 1 and 2 with the shifted feedback law (11). From this point onwards, we restrict our attention to the single input case, i.e., we assume that  $m = 1$ .

#### A. Properties of the shifted stabilizer

Let  $P_{\bar{u}}$  be the solution of (8) with  $v = \bar{u} = \mathbb{1}$  defined in (2). Then, the function  $\beta : [-u^-, u^+] \rightarrow [0, 1]$  defined as

$$\begin{aligned} \beta(u_e) &= \min\{u^- + u_e, u^+ - u_e\} \\ &= \begin{cases} u^- + u_e, & \text{for } u_e \in [-u^-, u_0] \\ u^+ - u_e, & \text{for } u_e \in [u_0, u^+] \end{cases} \end{aligned} \quad (17)$$

defines the maximal value  $\beta(u_e) = \kappa$  in Corollary 2 (with  $v = \bar{u}$ ) such that the assumptions of Corollary 2 are satisfied. Moreover, according to Corollary 1, the feedback law (11) guarantees the asymptotic stability of  $x_e(u_e)$  in (4), with basin of attraction containing the set

$$\mathcal{E}_{x_e(u_e)}^{\beta(u_e)}(P_{\bar{u}}) = \{x \in \mathbb{R}^n : |x - x_e(u_e)|_{P_{\bar{u}}} \leq \beta(u_e)\}. \quad (18)$$

In the  $\chi$ -coordinates, introducing  $\chi_e(u_e) := P_{\bar{u}}^{\frac{1}{2}} x_e(u_e)$  (see (16)), the set  $\mathcal{E}_{x_e(u_e)}^{\beta(u_e)}(P_{\bar{u}})$  simplifies to

$$\mathcal{E}_{\chi_e(u_e)}^{\beta(u_e)}(I) = \{\chi \in \mathbb{R}^n : |\chi - \chi_e(u_e)| \leq \beta(u_e)\}, \quad (19)$$

which we will work with in the following. In this section we will prove that the proposed scheduled law is stabilizing with basin of attraction containing the union of the sublevel sets generated by all possible values of  $u_e \in (-u^-, u^+)$ ,

$$\mathcal{R}_x = \bigcup_{u_e \in (-u^-, u^+)} \mathcal{E}_{x_e(u_e)}^{\beta(u_e)}(P_{\bar{u}}), \quad \mathcal{R}_\chi = \bigcup_{u_e \in (-u^-, u^+)} \mathcal{E}_{\chi_e(u_e)}^{\beta(u_e)}(I), \quad (20)$$

expressed in the  $x$ - and  $\chi$ -coordinates, respectively. Also with symmetric saturation limits,  $\mathcal{R}_x$  may provide a larger estimate of the basin of attraction than the ellipsoidal estimates of the form  $\mathcal{E}_0^{\beta(0)}(P_{\bar{u}})$ . For  $\chi \in \text{int}(\mathcal{R}_\chi)$  we consider the following optimization problem

$$\begin{aligned} u_e^*(\chi) &\in \underset{u_e \in [-u^-, u^+]}{\text{argmin}} \chi_e(u_e)^\top \chi_e(u_e) \\ &\text{subject to } |\chi - \chi_e(u_e)| \leq \beta(u_e). \end{aligned} \quad (21)$$

Based on a state  $\chi \in \text{int}(\mathcal{R}_\chi)$ , optimization problem (21) implicitly defines an induced equilibrium pair  $(\chi_e^*, u_e^*)$ , with

$$\chi_e^* = \chi_e(u_e^*) := P_{\bar{u}}^{\frac{1}{2}} x_e(u_e^*) = -C u_e^* := -P_{\bar{u}}^{\frac{1}{2}} A^{-1} B u_e^* \quad (22)$$

such that  $\chi \in \mathcal{E}_{\chi_e^*}^{\beta(u_e^*)}(I)$  holds. Moreover, the objective function is defined so that, from the set of feasible solutions, the one with the shortest distance to the origin is selected.

*Lemma 1:* Let  $m = 1$  and assume that Assumptions 1 and 2 are satisfied. Consider the optimization problem (21) where  $\beta$  and  $\mathcal{R}_\chi$  are defined in (17) and (20), respectively. Then the following properties are satisfied:

- 1) For all  $\chi \in \text{int}(\mathcal{R}_\chi)$ , (21) is feasible, the feasible set is closed and convex and its interior is nonempty;
- 2) The set-valued map  $F : \text{int}(\mathcal{R}_\chi) \rightrightarrows [-u^-, u^+]$ ,  

$$F(\chi) = \{u_e \in [-u^-, u^+] \mid |\chi - \chi_e(u_e)| \leq \beta(u_e)\},$$
defining the feasible set, is continuous;
- 3)  $u_e^*(\chi) = 0$  for all  $\chi \in \mathcal{E}_0^{\beta(0)}(I)$ ;
- 4)  $u_e^*(\chi)$  satisfies  $|\chi - \chi_e(u_e^*)| = \beta(u_e^*)$  for all  $\chi \in \text{int}(\mathcal{R}_\chi) \setminus \mathcal{E}_0^{\beta(0)}(I)$ ;
- 5)  $u_e^*(\chi) \in (-u^-, u^+)$  is unique for all  $\chi \in \text{int}(\mathcal{R}_\chi)$ ;
- 6)  $u_e^*(\cdot) : \text{int}(\mathcal{R}_\chi) \rightarrow (-u^-, u^+)$  is Lipschitz.  $\square$

*Proof:* **Item 1.** Feasibility follows immediately from the definitions of function  $\beta$  and the set  $\mathcal{R}_\chi$ . Moreover, since  $[-u^-, u^+]$  is non-empty, for each  $\chi \in \text{int}(\mathcal{R}_\chi)$ , there exists  $u_e \in (-u^-, u^+)$  satisfying  $\chi \in \text{int}(\mathcal{E}_{\chi_e(u_e)}^{\beta(u_e)}(I))$  and continuity of  $|\chi - \chi_e(\cdot)|$  and  $\beta(\cdot)$  imply the existence of  $\varepsilon > 0$  such that  $\chi \in \mathcal{E}_{\chi_e(u_e + \delta)}^{\beta(u_e + \delta)}(I)$ ,  $u_e + \delta \in (-u^-, u^+)$  whenever  $|\delta| \leq \varepsilon$ , namely the feasible set has nonempty interior. Closedness of the feasible set follows from continuity of  $|\chi - \chi_e(\cdot)|$  and  $\beta(\cdot)$  and the nonstrict inequality in (21). Let  $\chi \in \mathcal{R}_\chi$  and take  $u_{e_1}, u_{e_2} \in [-u^-, u^+]$  such that  $|\chi - \chi_e(u_{e_1})| \leq \beta(u_{e_1})$  and  $|\chi - \chi_e(u_{e_2})| \leq \beta(u_{e_2})$ . Then for all  $\lambda \in [0, 1]$ , using (16)

$$\begin{aligned} |\chi - \chi_e(\lambda u_{e_1} + (1 - \lambda)u_{e_2})| \\ \leq \lambda |\chi - \chi_e(u_{e_1})| + (1 - \lambda) |\chi - \chi_e(u_{e_2})| \\ \leq \lambda \beta(u_{e_1}) + (1 - \lambda) \beta(u_{e_2}) \leq \beta(\lambda u_{e_1} + (1 - \lambda)u_{e_2}). \end{aligned} \quad (23)$$

The last step follows from the concavity of  $\beta$  in (17). Thus, the feasible set is convex.

**Item 2.** Continuity of  $F$  follows from the properties established in item 1 together with [7, Example 3B.4] (or [7, Theorem 3B.3]). In particular, (23) shows that  $g(\chi, \cdot) = |\chi - \chi_e(\cdot)| - \beta(\cdot)$  is convex on the domain of interest.

**Item 3** follows from (19) and the objective function.

**Item 4.** To obtain a contradiction, assume that  $|\chi - \chi_e(u_e^*)| < \beta(u_e^*)$ . Since  $\chi \notin \mathcal{E}_0^{\beta(0)}(I)$  it follows that  $\chi_e(u_e^*) \neq 0$ , i.e.,  $u_e^* \neq 0$ . Since  $\beta(\cdot)$ ,  $\chi_e(\cdot)$  and  $|\cdot|$  are continuous, there exists  $u_e^\# \in [-u^-, u^+]$  with  $|u_e^\#| < |u_e^*|$  and  $|\chi - \chi_e(u_e^\#)| < \beta(u_e^\#)$ . Moreover, the condition  $|u_e^\#| < |u_e^*|$  implies that  $\chi_e(u_e^\#)^\top \chi_e(u_e^\#) < \chi_e(u_e^*)^\top \chi_e(u_e^*)$ , which contradicts the optimality of  $u_e^*$  and thus completes the proof.

**Item 5.** Since the feasible set is closed, convex and compact (see item 1) and the objective function is continuous, the minimum  $|\chi_e(u_e^*(\chi))|^2$  in (21) is attained through  $u_e^*(\chi) \in F(\chi) \subset [-u^-, u^+]$ . Moreover, since the objective function is strictly convex,  $u_e^*(\chi) \in (-u^-, u^+)$  is unique.

**Item 6.** Since  $F(\cdot)$  is continuous and due to the selection of the objective function,  $u_e^*(\cdot)$  is continuous (see [2, Ch. 1, Sec. 7, Thm. 1] and [1, Ch. 6.5.1]). As a next step consider  $u_1, u_2 \in (-u^-, u^+)$  and  $\chi_1, \chi_2 \in \text{int}(\mathcal{R}_\chi)$  with

$\chi_1 \in \mathcal{E}_{\chi_e(u_1)}^{\beta(u_1)}(I)$ ,  $\chi_2 \in \mathcal{E}_{\chi_e(u_2)}^{\beta(u_2)}(I)$ . For any  $\lambda \in [0, 1]$  consider the convex combinations

$$u_\lambda = \lambda u_1 + (1 - \lambda)u_2, \quad \chi_\lambda = \lambda \chi_1 + (1 - \lambda)\chi_2.$$

Then proceeding as in (23), we get

$$\begin{aligned} |\chi_\lambda - \chi_e(u_\lambda)| &= |\lambda(\chi_1 - \chi_e(u_1)) + (1 - \lambda)(\chi_2 - \chi_e(u_2))| \\ &\leq \lambda |\chi_1 - \chi_e(u_1)| + (1 - \lambda) |\chi_2 - \chi_e(u_2)| \leq \beta(u_\lambda), \end{aligned}$$

i.e.,  $\chi_\lambda \in \mathcal{E}_{\chi_e(u_\lambda)}^{\beta(u_\lambda)}(I)$  and  $\chi_\lambda \in \mathcal{R}_\chi$ . Consider any  $\chi_1, \chi_2 \in \text{int}(\mathcal{R}_\chi)$  and the corresponding optimal solutions  $u_e^*(\chi_1), u_e^*(\chi_2) \in (-u^-, u^+)$ . For any  $\lambda \in [0, 1]$  consider  $\chi_\lambda = \lambda \chi_1 + (1 - \lambda)\chi_2$ , the corresponding optimal solution of (21) denoted by  $u_e^*(\chi_\lambda)$  and the suboptimal solution  $\tilde{u}_\lambda = \lambda u_e^*(\chi_1) + (1 - \lambda)u_e^*(\chi_2)$  characterized above. From optimality, the square root of the objective function satisfies

$$\begin{aligned} |\chi_e(u_e^*(\chi_\lambda))| &\leq |\chi_e(\tilde{u}_\lambda)| \\ &\leq \lambda |\chi_e(u_e^*(\chi_1))| + (1 - \lambda) |\chi_e(u_e^*(\chi_2))|. \end{aligned}$$

In particular,  $|\chi_e(u_e^*(\cdot))| : \text{int}(\mathcal{R}_\chi) \rightarrow (-u^-, u^+)$  is a convex function and thus a locally Lipschitz continuous function (see [16, Thm. 10.4]), i.e., for each compact and convex set  $K \subset \text{int}(\mathcal{R}_\chi)$  there is  $L > 0$  such that

$$\begin{aligned} |C| \cdot \|u_e^*(\chi_1) - u_e^*(\chi_2)\| &= \|\chi_e(u_e^*(\chi_1)) - \chi_e(u_e^*(\chi_2))\| \\ &\leq L |\chi_1 - \chi_2| \quad \forall \chi_1, \chi_2 \in K. \end{aligned}$$

This estimate in particular implies that

$$|u_e^*(\chi_1) - u_e^*(\chi_2)| \leq \frac{L}{|C|} |\chi_1 - \chi_2| \quad \forall \chi_1, \chi_2 \in K$$

whenever  $u_e^*(\chi_1), u_e^*(\chi_2) \in [-u^-, 0]$  or  $u_e^*(\chi_1), u_e^*(\chi_2) \in [0, u^+]$ . As a last step, we define the functions  $\alpha^+ : \text{int}(\mathcal{R}_\chi) \rightarrow [0, u^+]$ ,  $\alpha^- : \text{int}(\mathcal{R}_\chi) \rightarrow [-u^-, 0]$ ,

$$\alpha^+(\chi) = \max\{u_e^*(\chi), 0\}, \quad \alpha^-(\chi) = \min\{u_e^*(\chi), 0\}$$

satisfying  $u_e^*(\chi) = \alpha^+(\chi) + \alpha^-(\chi)$  for all  $\chi \in \text{int}(\mathcal{R}_\chi)$ . Moreover, since  $u_e^*(\cdot)$  is continuous,  $\alpha^+(\cdot)$  and  $\alpha^-(\cdot)$  are continuous, and the estimate

$$\begin{aligned} |u_e^*(\chi_1) - u_e^*(\chi_2)| &= |\alpha^+(\chi_1) - \alpha^+(\chi_2) + \alpha^-(\chi_1) - \alpha^-(\chi_2)| \\ &\leq |\alpha^+(\chi_1) - \alpha^+(\chi_2)| + |\alpha^-(\chi_1) - \alpha^-(\chi_2)| \\ &\leq \frac{L}{|C|} |\chi_1 - \chi_2| + \frac{L}{|C|} |\chi_1 - \chi_2| \leq \frac{2L}{|C|} |\chi_1 - \chi_2| \end{aligned}$$

shows local Lipschitz continuity of  $u_e^*$ .  $\blacksquare$

## B. Stabilization with scheduled shifted coordinates

With Lemma 1 we are able to construct a control law stabilizing the origin from any initial condition satisfying  $x \in \text{int}(\mathcal{R}_x)$ . Recall that, through the coordinate transformation (15), there is a one to one mapping between  $x$  and  $\chi$ , therefore we can equivalently express the control law as a function of  $\chi$  or  $x$ . Opting for the formulation as a function of  $x$ , we can now state the main feedback controller proposed in this paper, combining the results of Corollary 2 and Lemma 1 together with Remark 1 for the case  $m = 1$  addressed here. The controller is given by the state feedback law

$$u = u_e^*(x) + K(x + A^{-1}Bu_e^*(x)) \quad (24)$$

+  $L(I - L)^{-1} dz_{[u^-, u^+]}(u_e^*(x) + K(x + A^{-1}Bu_e^*(x)))$ , defined through the optimal solution of (21). Based on Lemma 1, our main theorem proves its properties.

*Theorem 1:* Consider system (1) with  $m = 1$ , satisfying

Assumptions 1 and 2. Let  $u^-, u^+ \in \mathbb{R}_{>0}$ , let  $P_{\bar{u}}$  denote the solution of (8) for  $v = \bar{u}$  and  $\alpha > 0$  arbitrary. Then (24)

- 1) is well defined and Lipschitz for all  $x \in \text{int}(\mathcal{R}_x)$ ;
- 2) coincides with (5) for all  $x \in \mathcal{E}_0^{\beta(0)}(P_{\bar{u}})$  and thus locally preserves performance; and
- 3) asymptotically stabilizes the origin of (1) with basin of attraction containing  $\text{int}(\mathcal{R}_x)$ .  $\square$

*Proof:* The proof exploits Lemma 1. The equivalence between the coordinate representations  $\chi$  and  $x$  allows us to derive the results in the  $\chi$  coordinates.

**Item 1.** That (24) is well defined in  $\chi \in \text{int}(\mathcal{R}_\chi)$  and Lipschitz continuity of the feedback law follow from the corresponding properties in Lemma 1 and from Remark 1.

**Item 2.** First, through the second item in Lemma 1, in the set  $\mathcal{E}_0^{\beta(0)}(I)$ , the modified control law (24) and the original control law (5) coincide. Moreover, Proposition 1 implies that the origin is locally asymptotically stable, and  $\mathcal{E}_0^{\beta(0)}(I)$  is forward invariant and contained in the basin of attraction.

**Item 3.** We complete the proof by showing attractivity from  $\text{int}(\mathcal{R}_\chi)$ . To this end, we first show that for each pair  $\underline{w}, \bar{w} \in (-u^-, u^+)$ , with  $\underline{w} \leq 0 \leq \bar{w}$ , the set

$$\mathcal{R}_\chi^{\underline{w}, \bar{w}} = \bigcup_{u_e \in [\underline{w}, \bar{w}]} \mathcal{E}_{\chi_e(u_e)}^{\beta(u_e)}(I) \quad (25)$$

is forward invariant. Assume that  $\chi \in \partial \mathcal{R}_\chi^{\underline{w}, \bar{w}}$ ; i.e.,  $\chi$  is in the boundary of the set. Since  $0 \in [\underline{w}, \bar{w}]$  and since the distance of  $u_e$  to the origin is minimized through the objective function in (21), it holds that  $u_e^*(x) \in [\underline{w}, \bar{w}]$ . Thus, from Corollary 2 and the strict inequality in (13), the closed-loop vector field points to the interior of  $\mathcal{E}_{\chi_e(u_e^*(\chi))}^{\beta(u_e^*(\chi))}(I)$  and since  $\mathcal{E}_{\chi_e(u_e^*(\chi))}^{\beta(u_e^*(\chi))}(I) \subset \mathcal{R}_\chi^{\underline{w}, \bar{w}}$  it also points to the interior of  $\mathcal{R}_\chi^{\underline{w}, \bar{w}}$ . From continuity, forward invariance of  $\text{int}(\mathcal{R}_\chi^{\underline{w}, \bar{w}})$  follows. Now, let  $\chi(\cdot) : \mathbb{R}_{\geq 0} \rightarrow \text{int}(\mathcal{R}_\chi^{\underline{w}, \bar{w}})$  be a solution satisfying  $\chi(0) \in \text{int}(\mathcal{R}_\chi^{\underline{w}, \bar{w}})$ . If we define

$$\underline{w}(t) = \min\{u_e^*(\chi(t)), 0\}, \quad \bar{w}(t) = \max\{0, u_e^*(\chi(t))\}$$

then the forward invariance of  $\text{int}(\mathcal{R}_\chi^{\underline{w}(t), \bar{w}(t)})$  implies that  $|u_e^*(\chi(\cdot))|$  is monotonically decreasing.

Let us complete the proof by showing that  $\chi(t) \rightarrow 0$  for  $t \rightarrow \infty$ . Since  $u_e^*(\chi(\cdot))$  is Lipschitz continuous,  $u_e^*(\chi(\cdot))$  is differentiable for almost all  $t \in \mathbb{R}_{\geq 0}$ . For the sake of a contradiction, if  $\chi(t)$  does not converge to the origin, the set  $\mathcal{E}_0^{\beta(0)}(I)$  is not reached in finite time. This implies that (due to the monotonicity and boundedness of  $|u_e^*(\cdot)|$ )  $\dot{u}_e^*(\chi(t)) \rightarrow 0$  for  $t \rightarrow \infty$  (for almost all  $t \in \mathbb{R}_{\geq 0}$ ) and (due to the objective function of the optimization problem (21))  $|\chi(t) - \chi_e(u_e^*(t))| \rightarrow 0$  for  $t \rightarrow \infty$ . Lemma 1.4 implies that  $|\chi(t) - \chi_e(u_e^*(t))|^2 = \beta(u_e^*(t))^2$  and the time derivative satisfies

$$(\chi - \chi_e(u_e^*(\chi)))^\top (\dot{\chi} - \dot{\chi}_e(u_e^*(\chi))) = \beta(u_e^*) \frac{\partial \beta}{\partial u_e^*}(u_e^*) \dot{u}_e^*$$

for almost all  $t \in \mathbb{R}_{\geq 0}$ . Exploiting  $\dot{\chi}_e(u_e^*(\chi)) = -C \dot{u}_e^*(\chi)$  and using the decrease condition (13) for  $\langle \nabla V_{\chi_e}(\chi(t)), \dot{\chi}(t) \rangle$  this expression leads to the estimate

$$\left[ -(\chi - \chi_e(u_e^*(\chi)))^\top C + \beta(u_e^*) \frac{\partial \beta}{\partial u_e^*}(u_e^*) \right] \dot{u}_e^* < -\alpha |\chi - \chi_e(u_e^*)|^2$$
 for almost all  $t \in \mathbb{R}_{\geq 0}$ . Thus,  $\dot{u}_e^*(\chi(t)) \rightarrow 0$  for  $t \rightarrow \infty$ , leading to a contradiction and completing the proof.  $\blacksquare$

#### IV. EXPLICIT EXPRESSION OF THE STABILIZER

So far the feedback law (24) is only implicitly defined through the optimal solution of (21). In the single-input case, due to the simplicity of the optimization problem, a finite set of possible optimal solutions can be derived offline, from which the online/real-time computation of the control input becomes possible with low computational burden. To present the corresponding result we use the quantity  $C$  defined in (22) and define  $u_e^*$  in terms of  $\chi$  instead of  $x$ . Additionally, we define  $u_e^{\#i} \in \mathbb{C} \cup \{\pm\infty\}$ ,  $i \in \{1, \dots, 6\}$  with

$$u_e^{\#1}(\chi) = \frac{-|\chi|^2 + (u^-)^2}{2(\chi^\top C - u^-)}, \quad u_e^{\#2}(\chi) = \frac{-|\chi|^2 + (u^+)^2}{2(\chi^\top C + u^+)},$$

$$u_e^{\#3,4}(\chi) = \frac{\chi^\top C - u^- \pm \sqrt{(\chi^\top C)^2 - |C|^2 |\chi|^2 + |C u^- - \chi|^2}}{1 - |C|^2},$$

$$u_e^{\#5,6}(\chi) = \frac{\chi^\top C + u^+ \pm \sqrt{(\chi^\top C)^2 - |C|^2 |\chi|^2 + |C u^+ + \chi|^2}}{1 - |C|^2}.$$

*Theorem 2:* Let the assumptions of Theorem 1 be satisfied and consider the optimization problem (21) and  $C$  defined in (22). If  $|C| = 1$  define

$$\mathcal{S} = (\{u_e^{\#1}\} \cap [-u^-, u_0]) \cup (\{u_e^{\#2}\} \cap [u_0, u^+])$$

and for  $|C| \neq 1$  consider

$$\mathcal{S} = (\{u_e^{\#3}, u_e^{\#4}\} \cap [-u^-, u_0]) \cup (\{u_e^{\#5}, u_e^{\#6}\} \cap [u_0, u^+]).$$

Then, for  $\chi \in \text{int}(\mathcal{R}_\chi) \setminus \mathcal{E}_0^{\beta(0)}(I)$ , the optimal solution of (21) satisfies

$$u_e^*(\chi) \in \operatorname{argmin}_{u_e \in \mathcal{S}} |\chi_e(u_e)|^2, \quad (26)$$

while, for  $\chi \in \mathcal{E}_0^{\beta(0)}(I)$  it is given by  $u_e^* = 0$ .  $\square$

Note that the set  $\mathcal{S}$ , which can be easily constructed, contains at most 4 points. Thus, the optimal solution of (21) is obtained by calculating and comparing the objective values of  $u_e \in \mathcal{S}$  in (26).

*Proof:* The fact that  $u_e^*(\chi) = 0$  for  $\chi \in \mathcal{E}_0^{\beta(0)}(I)$  follows from Lemma 1, item 3. The six values  $u_e^{\#i}(\chi)$ ,  $i \in \{1, \dots, 6\}$  are obtained by solving the constraint

$$|\chi - \chi_e(u_e)|^2 = (\beta(u_e))^2 \quad (27)$$

of the optimization problem (21) for  $\beta(u_e) = u^- + u_e$  and  $\beta(u_e) = u^+ - u_e$  according to the definition of  $\beta$  in (17). Using an equality instead of the inequality in (27) is justified by Lemma 1, item 4. It follows from standard calculations that  $u_e^{\#i}(\chi)$ ,  $i \in \{1, 2\}$ , represent the solutions of (27) in the case  $|C| = 1$  while  $u_e^{\#i}(\chi)$ ,  $i \in \{3, \dots, 6\}$  are the solutions of (27) in the case  $|C| \neq 1$ . Then, the assertion follows by combining Lemma 1, items 1, 4 and 5.  $\blacksquare$

#### V. NUMERICAL ILLUSTRATION

*Example 2:* We continue with the setting discussed in Example 1. The closed-loop solutions using the feedback law (24) initialized at  $x_0 = [4.8 \ 3]^\top$  and  $x_0 = [-1.6 \ -0.96]^\top$  are shown in Fig. 3. The sets  $\mathcal{R}_x$  and  $\mathcal{R}_\chi$ , respectively, from which convergence to the origin is guaranteed are shown in cyan. The sets  $\mathcal{E}_0^{\beta(0)}(P_1)$  and  $\mathcal{E}_0^{\beta(0)}(I)$  (blue), correspond to the estimate of the basin of attraction obtained from the method in Proposition 1, while the sets  $\mathcal{E}_{x_e(u_0)}^{\beta(u_0)}(P_{\bar{u}})$  and  $\mathcal{E}_{\chi_e(u_0)}^{\beta(u_0)}(I)$  (green), show the enlarged estimate obtained by

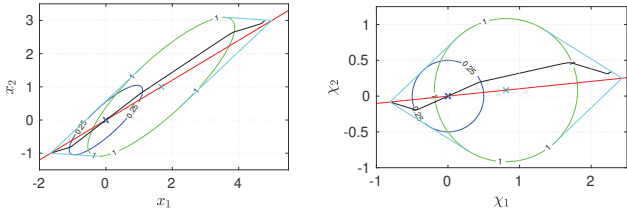


Fig. 3. Closed-loop solutions using the feedback law (24) converging to the origin (black). Additionally,  $\mathcal{R}_x$ ,  $\mathcal{R}_\chi$  (cyan),  $\mathcal{E}_0^{\beta(0)}(P_1)$ ,  $\mathcal{E}_0^{\beta(0)}(I)$  (blue),  $\mathcal{E}^{\beta(u_o)}(P_1)$ ,  $\mathcal{E}^{\beta(u_o)}(I)$  (green) and the subspace of induced equilibria  $\Gamma$  (red) are shown.

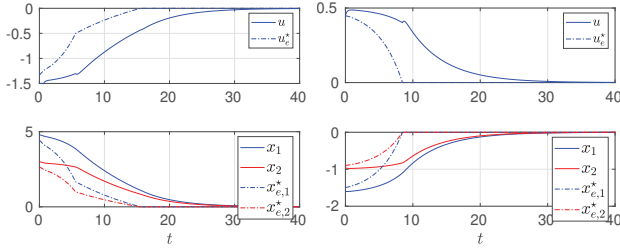


Fig. 4. Evolution of input  $u$ , state  $x$  and points  $u_e$  and  $x_e$  for the initial conditions  $x_0 = [4.8 \ 3]^T$  (left) and  $x_0 = [-1.6 \ -0.96]^T$  (right). The kink occurs when the slope of  $\beta(u_e)$  changes from increasing to decreasing (left) and when the state  $x$  enters the set  $\mathcal{E}_0^{\beta(0)}(P_1)$  (right).

the solution in [15], which however modifies the local performance. Our sets  $\text{int}(\mathcal{R}_x)$  and  $\text{int}(\mathcal{R}_\chi)$  clearly outperform both approaches. In particular, even though not represented in our figures, the solutions corresponding to the initial conditions  $x_0 = [4.8, 3]^T$  and  $x_0 = [-1.6, -0.96]^T$  using the original control law (5) are diverging. The time evolution of the input  $u$  and the state  $x$  is visualized in Fig. 4, which also shows the evolution of  $u_e^*(x)$  and  $x_e(u_e^*(x))$ .

*Example 3:* To illustrate that our solution applies with any state dimension  $n \in \mathbb{N}$ , consider plant (1) with

$$A = \begin{bmatrix} 0.6 & -0.8 & 0.3 \\ 0.8 & 0.6 & 0.5 \\ 1.0 & 0.3 & -1.0 \end{bmatrix} \quad \text{and} \quad B = \begin{bmatrix} 1 \\ 4 \\ 2 \end{bmatrix}. \quad (28)$$

Similar to the two-dimensional case in Figs. 3 and 4, estimates of the basin of attraction and a closed-loop solution are visualized in Fig. 5. The control law is again obtained by solving (8)<sup>2</sup> for  $v = 1$  and  $\alpha = 0.1$  and the saturation levels are defined as  $u^- = 1.5$  and  $u^+ = 0.5$ . The closed-loop solution shown in Fig. 5 is initialized at  $x_0 = [3.5 \ 1.5 \ 2.5]^T$ .

## VI. CONCLUSIONS

Through a suitably scheduled shift of the equilibrium, an enlarged estimate of the basin of attraction for bounded control laws with asymmetric saturations has been obtained. The control law is implicitly defined through an optimization problem. The focus on the single-input setting enables an illustrative interpretation of the controller design and allows for an explicit representation of the control law.

Future work will address the multi-input case and remove the assumption that  $A$  be non-singular, by directly representing  $\Gamma$  through the kernel of  $[A \ B]$ . To derive explicit solutions of (21) in the multi input setting, the

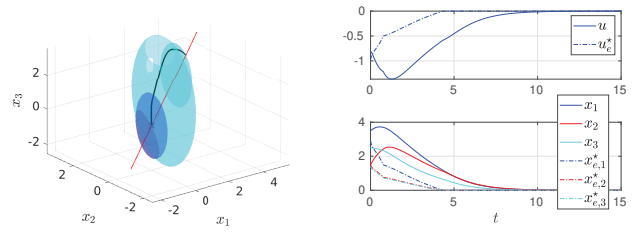


Fig. 5. Example 3: Estimates of the basin of attraction and a closed-loop solution using the feedback law (24) for dynamics (28).

<sup>2</sup>As in Example 1, the absolute values of the unknowns are constrained to be less than or equal to 10.

optimization problem may be reduced to a one dimensional subspace in the kernel of  $[A \ B]$ , depending on the state position. Alternatively, sample-and-hold approaches may be investigated, where  $(x_e^*, u_e^*)$  are only updated at discrete time steps.

## REFERENCES

- [1] J.-P. Aubin. *Viability Theory*. Birkhäuser, 1991.
- [2] J.-P. Aubin and A. Cellina. *Differential Inclusions: Set-Valued Maps and Viability Theory*. Springer, 1984.
- [3] A. Bemporad, M. Morari, V. Dua, and E. N. Pistikopoulos. The explicit linear quadratic regulator for constrained systems. *Automatica*, 38(1):3–20, 2002.
- [4] A. Benzaouia. Constrained stabilization: an enlargement technique of positively invariant sets. *IMA Journal of Mathematical Control and Information*, 22(1):109–118, 2005.
- [5] A. Benzaouia, F. Mesquine, and M. Benhayoun. *Saturated Control of Linear Systems*. Springer, 2017.
- [6] F. Blanchini and S. Miani. Any domain of attraction for a linear constrained system is a tracking domain of attraction. *SIAM Journal on Control and Optimization*, 38(3):971–994, 2000.
- [7] A. L. Dontchev and R. T. Rockafellar. *Implicit Functions and Solution Mappings*. Springer, 2009.
- [8] A. Grancharova and T. A. Johansen. *Explicit Nonlinear Model Predictive Control: Theory and Applications*, volume 429. Springer Science & Business Media, 2012.
- [9] M. Grant and S. Boyd. CVX: Matlab software for disciplined convex programming, version 2.1. <http://cvxr.com/cvx>, 2014.
- [10] B.L. Groff, J.M. Gomes da Silva Jr, and G. Valmorbidia. Regional stability of discrete-time linear systems subject to asymmetric input saturation. *IEEE Conf. on Decision and Control*, pages 169–174, 2019.
- [11] T. Hu and Z. Lin. *Control systems with actuator saturation: analysis and design*. Springer Science & Business Media, 2001.
- [12] T. Hu, A.N. Pitsillides, and Z. Lin. Null controllability and stabilization of linear systems subject to asymmetric actuator saturation. In *IEEE Conf. on Decision and Control*, pages 3254–3259, 2000.
- [13] T. Hu, A.N. Pitsillides, and Z. Lin. Null controllability and stabilization of linear systems subject to asymmetric actuator saturation. In V. Kapila and K. Grigoriadis, editors, *Actuator Saturation Control*, chapter 1, pages 47–76. Marcel Dekker, 2002.
- [14] Y. Li and Z. Lin. An asymmetric Lyapunov function for linear systems with asymmetric actuator saturation. *International Journal of Robust Nonlinear Control*, 21(4):1–17, 2017.
- [15] S. Mariano, F. Blanchini, S. Formentin, and L. Zaccarian. Asymmetric state feedback for linear plants with asymmetric input saturation. *IEEE Control Systems Letters*, 4(3):608–613, 2020.
- [16] R. T. Rockafellar. *Convex Analysis*. Princeton University Press, 1970.
- [17] S. Tarbouriech, G. Garcia, J.M. Gomes da Silva Jr., and I. Queinnec. *Stability and stabilization of linear systems with saturating actuators*. Springer-Verlag London Ltd., 2011.
- [18] C. Yuan and F. Wu. Switching control of linear systems subject to asymmetric actuator saturation. *International Journal of Control*, 88(1):204–215, 2015.